



## 저작자표시-비영리-변경금지 2.0 대한민국

이용자는 아래의 조건을 따르는 경우에 한하여 자유롭게

- 이 저작물을 복제, 배포, 전송, 전시, 공연 및 방송할 수 있습니다.

다음과 같은 조건을 따라야 합니다:



저작자표시. 귀하는 원저작자를 표시하여야 합니다.



비영리. 귀하는 이 저작물을 영리 목적으로 이용할 수 없습니다.



변경금지. 귀하는 이 저작물을 개작, 변형 또는 가공할 수 없습니다.

- 귀하는, 이 저작물의 재이용이나 배포의 경우, 이 저작물에 적용된 이용허락조건을 명확하게 나타내어야 합니다.
- 저작권자로부터 별도의 허가를 받으면 이러한 조건들은 적용되지 않습니다.

저작권법에 따른 이용자의 권리는 위의 내용에 의하여 영향을 받지 않습니다.

이것은 [이용허락규약\(Legal Code\)](#)을 이해하기 쉽게 요약한 것입니다.

[Disclaimer](#)

**Master's Thesis of Engineering**

**Development of a Kicking Detection  
Algorithm for Extracorporeal  
Membrane Oxygenation**

**체외막산소화장치에서의 킥 감지  
알고리즘 개발**

**February 2018**

**Interdisciplinary Program in Bioengineering  
The Graduate School  
Seoul National University**

**Hyun Soo Kim**

# 체외막산소화장치에서의 키팅 감지 알고리즘 개발

지도교수 이 정 찬

이 논문을 공학석사 학위논문으로 제출함

2018년 1월

서울대학교 대학원  
협동과정 바이오엔지니어링 전공  
김 현 수

김현수의 공학석사 학위논문을 인준함

2018년 1월

위 원 장	<u>김 희 찬</u>	(인)
부 위 원 장	<u>이 정 찬</u>	(인)
위 원	<u>최 영 빈</u>	(인)

**Development of a Kicking Detection  
Algorithm for Extracorporeal  
Membrane Oxygenation**

*Academic adviser* Jung Chan Lee

**Submitting a master's thesis of Engineering  
January 2018**

**Interdisciplinary Program in Bioengineering  
Graduate School, Seoul National University**

**Hyun Soo Kim**

**Confirming the master's thesis written by Hyun Soo Kim  
January 2018**

**Chair**

---

*Hee Chan Kim, Ph.D.*

**Vice Chair**

---

*Jung Chan Lee, Ph.D.*

**Examiner**

---

*Young Bin Choy, Ph.D.*

## **Abstract**

# **Development of a Kicking Detection Algorithm for Extracorporeal Membrane Oxygenation**

Hyun Soo Kim

Seoul National University Graduate School  
Interdisciplinary Program in Bioengineering

Extracorporeal membrane oxygenation (ECMO) is an extracorporeal technique to provide both cardiac and respiratory support to person whose heart and lungs are unable to supply an adequate amount of gas exchange to sustain life. Kicking phenomenon which is the blockage of the drainage cannula creates instant vacuum in the pump which causes cavitation, hemolysis and drop in pumping efficiency. Studies of suction detection on ECMO system seems to be insufficient since previous studies of suction detection algorithms have mostly focused on implantable blood pumps such as total artificial heart (TAH) and ventricular assist devices (VAD).

The purpose of this research was to develop an algorithm which detect kicking phenomenon

such as inlet pressure, flow rate, rotating speed and current consumption of rotating motor of the pump were selected as candidates for kicking detection indicators. The data of the candidate parameters were collected for 24 hours from veno-arterial ECMO operation to a female pig. The correlation between acquired data from ECMO device and the kicking data earned with acceleration data of drainage circuit were analyzed by evaluating confusion matrix of models attained by machine learning algorithm.

Motor current consumption data has outperformed other parameters over than 50% in terms of sensitivity and precision. Various algorithms were developed using the current consumption data. The algorithm using standard deviation was selected as the final kicking detection algorithm by showing better detection ability than the other detection algorithms in various *in vitro* experimental conditions. The suggested algorithm showed 97% accuracy when applied to the actual kicking data.

Motor current consumption data which the suggested algorithm adopted, has as several advantages other than accuracy of the algorithm itself. Other parameters such as drainage pressure and flow rate require additional sensors on the ECMO circuit, while it is unnecessary to equip any additional sensors utilizing motor current data. Also, motor current data acquisition is never disrupted unless the motor turns off.

Although there remain some limitations in the present study, the results light up the potential of further studies on suction detection system in terms of ECMO operations.

---

Keyword : Cardiopulmonary support system, Extracorporeal membrane oxygenation (ECMO), Suction detection, Machine learning, Mock circulation system

Student Number : 2016-21168

# Table of Contents

<b>Abstract .....</b>	<b>i</b>
<b>Table of Contents .....</b>	<b>iii</b>
<b>List of Tables .....</b>	<b>v</b>
<b>List of Figures .....</b>	<b>iii</b>
<b>List of Abbreviations .....</b>	<b>vii</b>
<b>Chapter 1. Introduction .....</b>	<b>1</b>
1.1 Mechanical Circulatory Support (MCS) .....	1
1.2 Extracorporeal Membrane Oxygenation (ECMO) .....	3
1.2.1 Background .....	3
1.2.2 Components of ECMO .....	4
1.2.3 VA&VV ECMO .....	6
1.2.4 Kicking phenomenon .....	8
1.3 Related works .....	9
1.4 Current limitations .....	10
1.5 Research aims .....	10
<b>Chapter 2. Method .....</b>	<b>11</b>
2.1 <i>In vivo</i> experiment conditions .....	11
2.2 Data acquisition .....	13
2.3 <i>In vitro</i> mock circulation system .....	15
2.4 Algorithm development .....	19
2.4.1 KNN algorithm .....	19
2.4.2 Confusion matrix .....	22

2.4.3 Parameter decision .....	25
2.4.4 Algorithm decision .....	28
2.4.4.1 Standard deviation algorithm .....	28
2.4.4.2 Minmax algorithm .....	29
2.4.4.3 Differential algorithm .....	29
2.4.5 Window problem .....	30
<b>Chapter 3. Result .....</b>	<b>31</b>
3.1 <i>In vivo</i> experiments results .....	31
3.2 Correlation comparison .....	33
3.3 <i>In vitro</i> evaluation .....	35
3.4 The suggested algorithm .....	42
<b>Chapter 4. Discussion .....</b>	<b>44</b>
4.1 Algorithm validation .....	44
4.2 Feasibility of the algorithm on ECMO devices .....	47
4.3 Limitations of the study .....	48
<b>Chapter 5. Conclusion .....</b>	<b>50</b>
References .....	51
Abstract in Korean .....	56

## **List of Tables**

Table 3-1. Confusion matrix outcomes .....	34
Table 3-2. Algorithm evaluation results during different kicking stages .....	41
Table 4-1. Confusion matrix outcomes of the suggested kicking detection algorithm .....	46

## List of Figures

Figure 1-1. Mechanical circulatory support systems .....	2
Figure 1-2. Schematic of ECMO circuit .....	5
Figure 1-3. Veno-Arterial (VA) & Veno-Venous (VV) ECMO .....	7
Figure 2-1. Components of in-vivo experiment .....	12
Figure 2-2. Data acquisition devices .....	14
Figure 2-3. Mock circulation system .....	17
Figure 2-4. Waveforms of kicking phenomenon from <i>in vitro</i> mock circulation system .....	18
Figure 2-5. K-nearest neighbor (K-NN) algorithm .....	21
Figure 2-6. Confusion matrix .....	24
Figure 2-7. Parameter decision process .....	26
Figure 3-1. <i>In vivo</i> experiment data outcomes .....	32
Figure 3-2. Confusion matrix of the candidate parameters .....	34
Figure 3-3. Kicking data acquired from mock circulation system .....	37
Figure 3-4. Algorithm application results during mild kicking stage .....	38
Figure 3-5. Algorithm application results during moderate kicking stage .....	39
Figure 3-6. Algorithm application results during severe kicking stage .....	40
Figure 3-7. Block diagram of the suggested algorithm .....	43
Figure 4-1. <i>In vivo</i> experiment data application results of suggested kicking detection algorithm .....	45
Figure 4-2. Confusion matrix of detection results using suggested kicking detection algorithm .....	46

## **List of Abbreviations**

ECMO	Extracorporeal Membrane Oxygenation
ECLS	Extracorporeal Life Support
TAH	Total Artificial Heart
VAD	Ventricular Assist Device
LVAD	Left Ventricular Assist Device
IABP	Intra-Aortic Blood Pump
CPB	Cardiopulmonary Bypass
MCS	Mechanical Circulatory Support
PMP	Polymethylpentene
K-NN	K-Nearest Neighbor
RBC	Red Blood Cell

# Chapter 1. Introduction

## 1.1 Mechanical Circulatory Support (MCS)

Mechanical circulatory support is lifesaving technology to the patients with severe heart failures such as cardiogenic shock, myocardial dysfunction, myocarditis and chronic heart failure [1]. After numerous clinical and technical development, MCS is now widely available for the patients. There are several modalities of MCS that have unique characteristics.

Figure 1-1 show the existing MCS modalities divided into two large groups by the period of use. Short term support devices are used to support patients for days to weeks. Intra-aortic balloon pump (IABP) is commonly used as the first treatment of cardiogenic shock. It operates based on counterpulsation which supports hemodynamics by diastolic pressure augmentation. Another representative short term MCS is extracorporeal membrane oxygenation (ECMO). ECMO not only circulates blood but also supplies oxygen to the blood in order to support both heart and lungs. Cardiopulmonary bypass (CPB) is a similar technique that temporarily takes over the function of both heart and lungs, but it is focused mainly on surgery situations.

Long term support devices are devices that are implantable or percutaneous to permanently replace or assist heart's functions. Ventricular assist device (VAD) is a pump that supports functions of the left, right or both heart ventricles. Particularly, VAD that supports left ventricle which pumps blood to most of the body is called left ventricular assist device (LVAD). Total Artificial Heart (TAH) is a form of a MCS which is explanted to the patient and replaces ventricles and valves of them. Currently, TAH is used in end-stage biventricular heart failure to

bridge the time to heart transplantation [2].

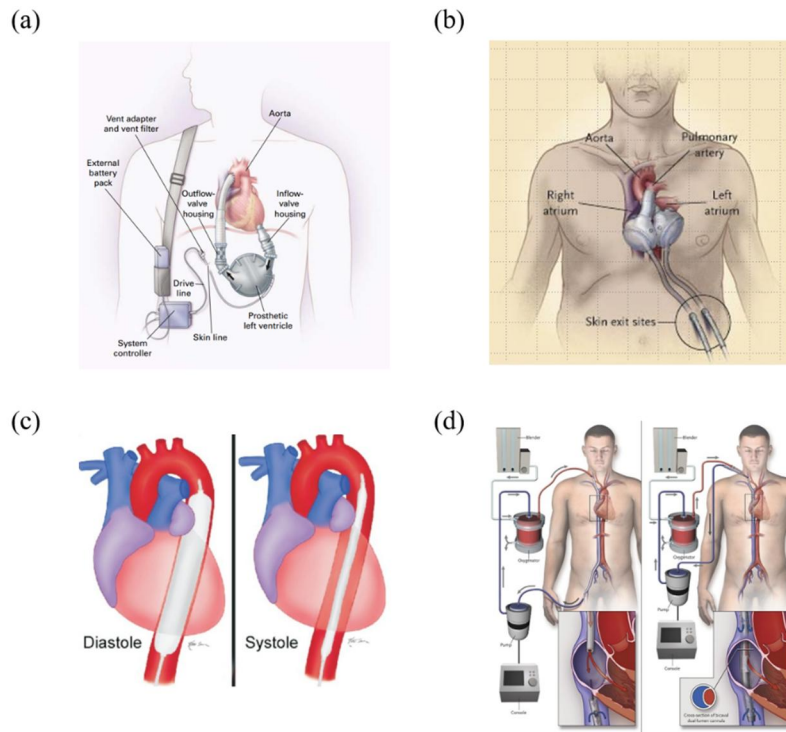


**Figure 1-1. Mechanical circulatory support systems**

(a) Ventricular assist device (VAD) [3] (b) Total artificial heart (TAH) [4] (c) Intra-aortic balloon pump [5] (d) Extracorporeal membrane oxygenation (ECMO) [6]

## 1.2 Extracorporeal Membrane Oxygenation (ECMO)

Extracorporeal membrane oxygenation (ECMO), also known as extracorporeal life support (ECLS), is an extracorporeal technique to provide both cardiac and respiratory support to person whose heart and lungs are unable to supply an adequate amount of gas exchange to sustain life. There is an increasing application of ECMO technology over the recent years [7]. This research aims to develop an algorithm that improves performance of ECMO devices.

### 1.2.1 Background

In 1944, Kolff and Berk found out blood became oxygenated passing through cellophane chambers of their artificial kidney [8]. The concept gave an idea to Gibbon who applied artificial oxygenation and perfusion support for the first successful open heart operation in 1953 [9]. Researches of various mechanical ventilation methods kept on improving further on. ECMO made a meteoric rise with an incident that shook the world. When novel swine-origin influenza A(H1N1) virus rapidly led to a worldwide pandemic in 2009, ECMO drew a great interest as an effective solution of severe respiratory failures. From then on, ECMO has become even more reliable with improving equipment, and increased experience, which led to improving results. ECMO development closely relates to rapid development of various medical technologies including clinically useful extracorporeal biocompatible blood pumps and membrane oxygenators.

### 1.2.2 Components of ECMO

Essential components of an ECMO system incorporate a blood pump, tubing, membrane oxygenator, medical oxygen blended sweep gas supplier and blood heat exchanging element. The schematic of the ECMO circuit configuration is shown in Figure 1-2.

Blood pump which rotates blood throughout the whole body and support heart's function is the most important part of ECMO. Conventionally, servo-regulated occlusive roller pump had been the most common type of ECMO blood pumps. However centrifugal type blood pump has shown to be effective and safe enough to meet the requirements of ECMO blood pump [10, 11]. Therefore, it became the general pump type for ECMO recently. Technical advances of the ECMO blood pump has continued in the field of coating materials for the surfaces, shape and number of impeller blades, slope and volume of the housing and rotor rotation speed [12].

Oxygenator supplies oxygen and removes carbon dioxide from blood to support function of the lung. It has developed from classical silicone rubber membrane lungs to hollow fiber polymethylpentene (PMP) oxygenators which are extremely efficient in respect of gas change with minimal plasma leakage [13].

From the first development of heart-lung bypass, blood warming devices were accompanied to maintain the patient's normal temperature. Blood is exposed to a large surface area resulting in a significant heat loss during the operation of ECMO. Therefore, heat exchange unit requires capacity for a large caloric exchange. Also, the temperature of the blood should be increased without significant damage to the blood element with minimal surface in contact [14, 15].

Additional components that can improve ECMO include venous and arterial pressure

monitoring device, anticoagulation monitoring equipment, emergency pump in case of primary blood pump failure or power failure, bubble detector and monitors for blood flow rate, circuit blood temperature, blood gas and oxygen saturation.

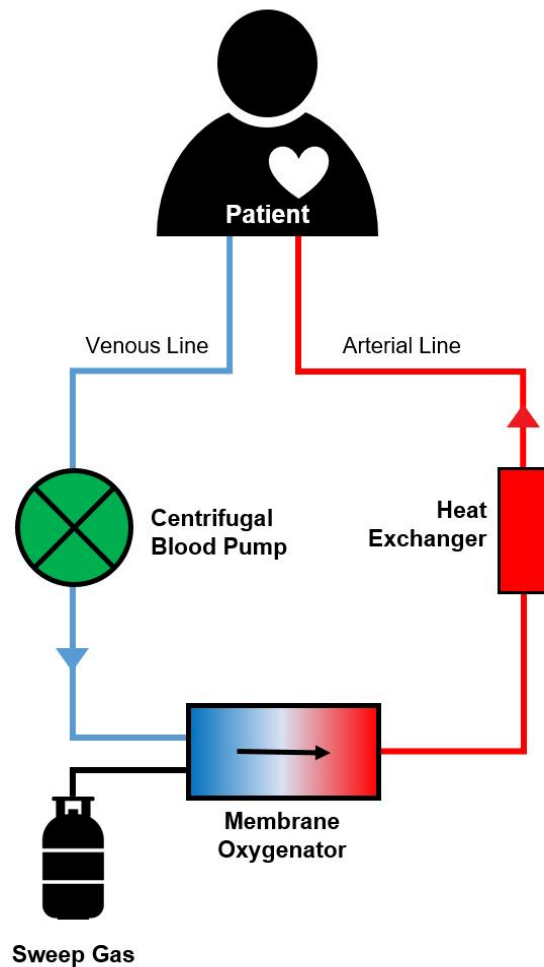


Figure 1-2. Schematic of ECMO circuit

Blood pump, tubing, membrane oxygenator, medical oxygen blended sweep gas supplier

and blood heat exchanging element are the essential components of ECMO.

### 1.2.3. Veno-Arterial (VA) & Veno-Venous (VV) ECMO

There are 2 different forms of ECMO modes depending on their clinical applications. The difference between them emerges by circuit configuration and how the system is connected to the patient [16]. Since Veno-Arterial (VA) ECMO provides both respiratory and hemodynamic support, the ECMO circuit here is connected in parallel to the heart and lungs, while in Veno-Venous (VV) ECMO the circuit is connected in series to the heart and lungs [17]. Schematics of both VV ECMO and VA ECMO is shown in Figure 1-3.

VA ECMO can be applied to patients suffering from either cardiac or respiratory insufficiency. It drains out blood from the right atrium through a cannula inserted into right internal jugular vein and returns into arterial system through ascending aorta. It reduces preloads of both ventricles and has better oxygen delivery compared to VV ECMO. But it increases post-load of left ventricle and reduces pulse pressure which may result in a pulseless circulation.

VV ECMO is applied to patients who need respiratory support. It carries out blood from inferior vena cava by means of a cannula inserted through femoral vein. After oxygenation of the blood, it is pumped into the right atrium through another cannula inserted into right jugular vein or contralateral femoral vein. Since it drains and re-infuses into the same venous line, it has an advantage to use a dual-lumen cannula that has both drainage and re-infusion lumens in a single cannula. But the adjacency of the two different catheter tips leaves possibilities of blood recirculation.

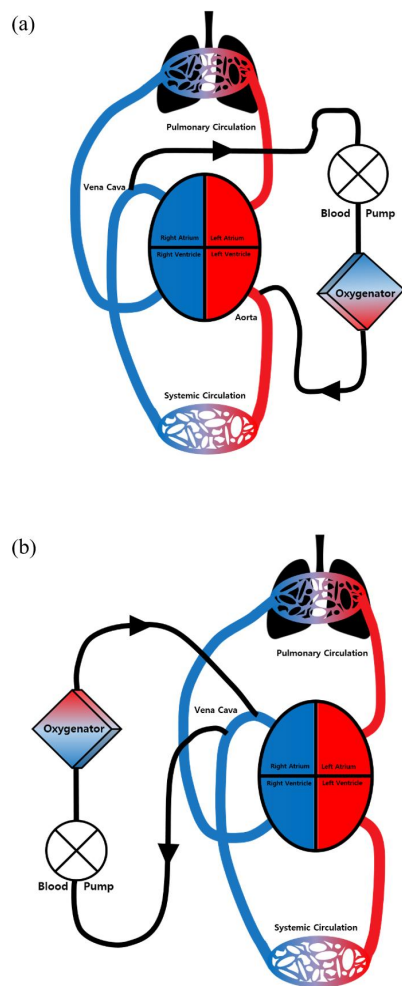


**Figure 1-3. Veno-Arterial (VA) & Veno-Venous (VV) ECMO**

- (a) Schematic of VA ECMO mode. VA ECMO can support function of both heart and lungs.
- (b) Schematic of VV ECMO mode. VV ECMO can support function of lungs.

#### 1.2.4 Kicking phenomenon

The amount of blood circulation of ECMO depends largely on patient's total blood volume. Excessive venous drainage, hypovolemia or cannula malposition leads to periodical shaking of the inlet line of the circuit, also noted as “kicking” or “chattering”. The kicking phenomenon occurs because the cava/atrium is collapsed and being sucked down on the venous cannula tip. The phenomenon results in an abrupt decrease in inlet pressure and fluctuation of circuit flow [18]. Also, the blockage creates instant vacuum in the pump which causes cavitation, hemolysis and drop in pumping efficiency [19, 20]. Therefore, an immediate reaction is required at the occurrence of the kicking phenomenon. There are several options to be made in the situation. Clinicians should ensure circuit patency, reposition drainage cannula and temporarily reduce pump's rotating speed. Another response has been to inject fluid, or for the patients of a hematocrit of less than 40%, to infuse packed red blood cells [21]. In the case, increase of 10% body weight secondary to fluid accumulation can lead to increased mortality [22]. In the worst cases, another venous catheter may be placed if sufficient blood flow cannot be obtained despite the above treatments.

### 1.3 Related works

There have been several studies of suction detection methods using various parameters of a blood pump particularly in the field of implantable blood pumps such as TAH and VAD. Ventricular collapse in the result of suction (over-pumping) or regurgitation (pump back flow) due to under-pumping is the harmful situations during implantable blood pump operations [23, 24]. Among the situations, suction event is the most hazardous state that must be detected immediately or else the cardiac muscle can be damaged. Since additional equipment of sensors is limited for implantable blood pumps, motor current has greatly interested many researchers having benefit of sensorless monitoring of the implantable blood circulation systems. Decreasing pump flow rate after detecting the occurrence of suction and regurgitation analyzing spectral density of motor current waveforms was proposed by Yuhki et al. [25] and Fu et al. [26] Applying different parameter other than motor current, Saito et al. [27] developed a suction control system using an implantable pressure sensor on the pump. The pressure sensor method had advantages of not only suction detection but also synchronization of natural heartbeat.

## 1.4 Current limitations

Studies of suction detection on ECMO system seems to be insufficient since previous studies of suction detection algorithms have mostly focused on implantable blood pumps such as TAH and VAD. But the kicking phenomenon of ECMO occurs mainly by vein collapse while sucking event of VAD occurs due to ventricular collapse. Also, afterload of the pumps directly affects VAD but not with ECMO due to the existence of an oxygenator. Therefore, waveforms of parameters such as motor current, pressure, motor rotating speed and flowrate between the both implantable blood pumps and ECMO would be different. Thus, there is a need of own suction detection system of ECMO.

## 1.5 Research aims

The purpose of this research was to develop an algorithm which detect kicking phenomenon situations during operation of ECMO. First, various data of parameters such as inlet pressure, flow rate, rotating speed and current consumption of rotating motor of the pump were recorded to determine the parameter that best reflects the moment of kicking phenomenon using machine learning algorithm since there were no studies of correlation between various values of parameters of ECMO pump and kicking phenomenon. Kicking detection algorithm was developed based on the decided parameter.

## **Chapter 2. Materials and Methods**

### **2.1 In-vivo experiment conditions**

VA mode ECMO was performed to a 70kg female pig at Bundang Seoul National University preclinical experiment center. The experimental ECMO circuit consisted of five elements. Prototype of a newly designed centrifugal blood pump was fabricated with double pivot bearing structures. The centrifugal blood pump which alternates heart's functions continuously rotated at speed around 3000 revolutions per minute for 24 hours to circulate blood at flow rate of 2.5 liters per minute. An oxygenator (Affinity NT Trillium Biosurface, Medtronic, USA) was equipped to provide adequate amount of oxygen to the blood in place of lungs. In order to maintain the body temperature, a heat exchange unit (Stockert Heater-Cooler System 3T, Sorin Group, USA) was applied. Body temperature was perfectly preserved to normothermia (37.5 °C). The experiment continued for 24 hours and blood samples were taken every hour to check the pig's status such as pH, pCO<sub>2</sub>, pO<sub>2</sub>, hematocrit percentage, lactate levels, etc. Also, blood coagulation level was measured at the same time

using microcoagulation system (Hemochron Signature Plus, International Technidyne Corporation, USA). Depending on the levels of anti-coagulation time, moderate amount of heparin was medicated. Pictures of the products utilized in the experiment are shown in Figure 2-1.

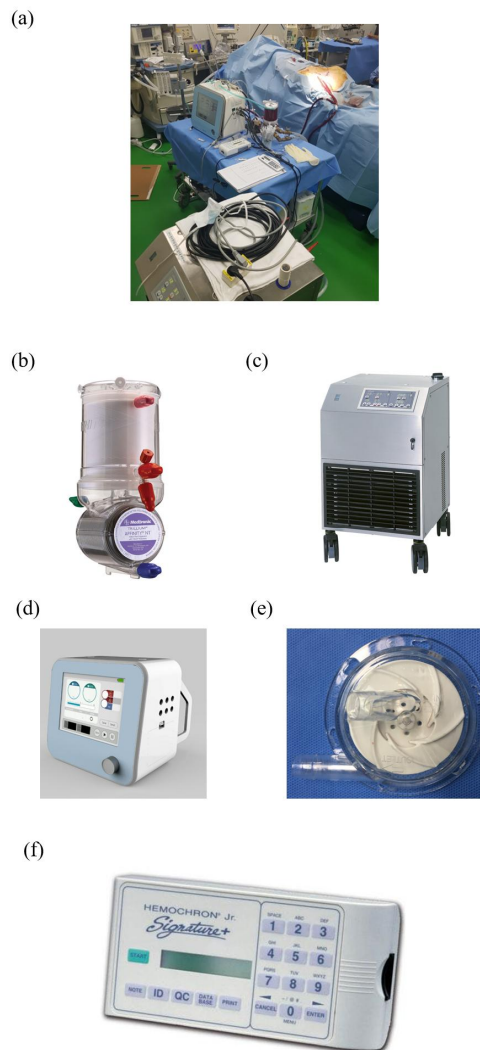


**Figure 2-1. Components of in-vivo experiment**

(a) In-vivo experiment was carried out at Bundang Seoul National University preclinical

experiment center. Experiment configurations consist of (b) an oxygenator (Affinity NT Trillium Biosurface), (c) a heat exchange unit (Stockert Heater-Cooler system 3T), (d) a developed ECMO device (SACSS), (e) a centrifugal blood pump, (f) a microcoagulation system (Hemochron Signature Plus).

## 2.2 Data acquisition

The developed ECMO device integrates sensors for three pressure parameters (HSCDANT030PDSA5, Honeywell Inc., Indiana, USA), temperature sensor (DTPML-SPI-81, DWELLSHOP, Gunpo Korea), flow sensor module (Transonic TS410, New York, USA), bubble detector (ABD06-L, New York, USA), brushless DC motor (EC-i40 70W, Maxon Motor, Sachseln, Switzerland) with its driving unit (ESCON 50/5, Maxon Motor, Sachseln, Switzerland). Data from three parameters - flow rate, pressure, RPM - were obtained from the ECMO device at sampling rates of 5Hz. And motor current data was collected by additional external ammeter (JTOOL-TESTER-1, JTOOL, Seongnam, Korea) using shunt resistors at a sampling rate of 16Hz. And finally because kicking phenomenon accompanies regular shaking of venous line of ECMO circuit, an accelerometer (Accelerometer Sensor #1, Kong-Tech, Seongnam, Korea) was fixed at the inlet line of the ECMO pump to detect the exact moment of kicking phenomenon. The data was defined as golden standard data to compare the data measured from the ECMO device with the moment of kicking phenomenon. The accelerometer data were sent to Arduino MEGA 2560 (Smart Projects, Ivrea, Italy) using SPI communication, and Labview software (National Instruments, Austin, USA) received each x, y and z-axis acceleration data from the Arduino device with serial communication at a sampling rate of 55Hz. All the above data were recorded throughout the experiment for 24 hours.

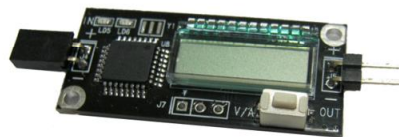
(a)



(b)



(c)



(d)



(e)



**Figure 2-2. Data acquisition devices**

Various measurement sensors were applied for data collection. (a) Motor and its driving unit

(b) Pressure sensor (c) Current measurement device (d) Flowmeter (e) Accelerometer

## 2.3 In-vitro mock circulation system

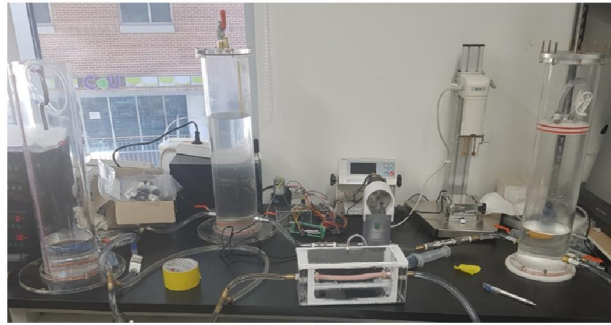
In-vitro mock circulation loop was developed in order to validate the algorithm that was developed based on the in-vivo experiment data. *In vitro* experiments have the advantage of being able to acquire results while changing various experimental conditions. Therefore, a developed algorithm can be validated in various different conditions adjusted in mock circulation system.

The developed mock circulation loop constitutes of five main compartments that represents ECMO operating condition. A pulsatile pump was applied to represent heart's function and two check valves were equipped in order to mimic mitral valve and semilunar valve that prevents regurgitation during pumping procedure and a chamber was linked after the pulsatile pump to represent left ventricular compliance. During positive pressure ventilation operations, inferior vena cava diameter is minimal on expiration and maximal on inspiration due to increase of pleural pressure [28, 29]. On the basis of the theory, an extravascular model was designed to replicate the effect of positive pressure ventilation effects on intravascular pressure. The extravascular model is comprised of venous drainage catheter inserted in a silicone vein model inside a vacuum box. The extravascular vacuum box was placed after left ventricular compliance chamber to control kicking phenomenon by injecting and ejecting air pressure in the box to change intravascular pressure of the silicone vein model. Venous drainage catheter was connected to ECMO blood pump and the outlet was connected to back to the initial

pulsatile pump through right atrium compliance chamber. To sum up, there are innumerable complicated physiological phenomenon intertwined with occurrences of kicking events. But fundamentally, kicking event occurs when incoming flow from the heart is insufficient compared to drainage flow of the ECMO device. The suggested mock circulation system mimicked venous collapse caused by the excessive drainage occurred during kicking situations. Finally, water and a 37% aqueous glycerol solution was circulated on the suggested mock system referring to the studies of centrifugal blood pumps on mock loop [30]. Viscosity of the 37% glycerol water solution was measured with vibrational viscometer (SV-10, A&D Company Ltd., Tokyo, Japan). The measured viscosity condition during the *in vitro* experiment was 1.92cp in 25.8°C. *In vitro* experiment data were collected with the exact same method of *in vivo* experiment data acquisition as mentioned in section 2.2. Schematic image of the developed mock circulation system is shown in Figure 2-3.

While it is uncertain whether the kicking phenomenon will occur in the actual *in vivo* experiment, the most valuable aspect of the mock circulation system is that it can reproduce kicking phenomenon anytime with desired intensities. *In vitro* mock circulation system was applied to evaluate the algorithm in various circumstances that can be occurred in actual ECMO operations. Kicking phenomena were categorized into three different groups by the acceleration intensity levels during kicking events. It was classified as mild kicking stage when the acceleration level was 0.08 g or less, which is a slight trembling that can be seen just before kicking occurs in earnest. Also, it was classified as moderate kicking stage when the acceleration level was in the range of 0.08 to 0.16 g which accompanies a noticeable shaking of the circuit as the kicking phenomenon progresses. Finally, it was classified as severe kicking stage when the acceleration level reached 0.16 g or more. Violent tremors can be observed at the instance of severe kicking and instant reaction is needed at the stage. Figure 2-4 shows each waveforms of three categorized kicking stages.

(a)



(b)

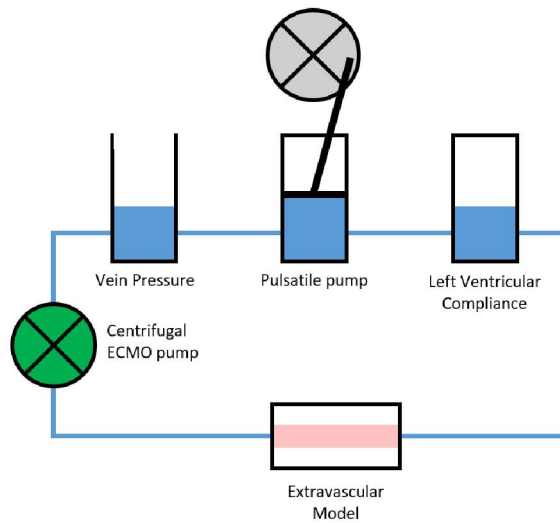


**Figure 2-3. Mock circulation system**

Mock circulation system was composed for kicking detection algorithm validation. (a)

Actual experimental settings of the mock circulation system. (b) Schematic of the mock circulation system.

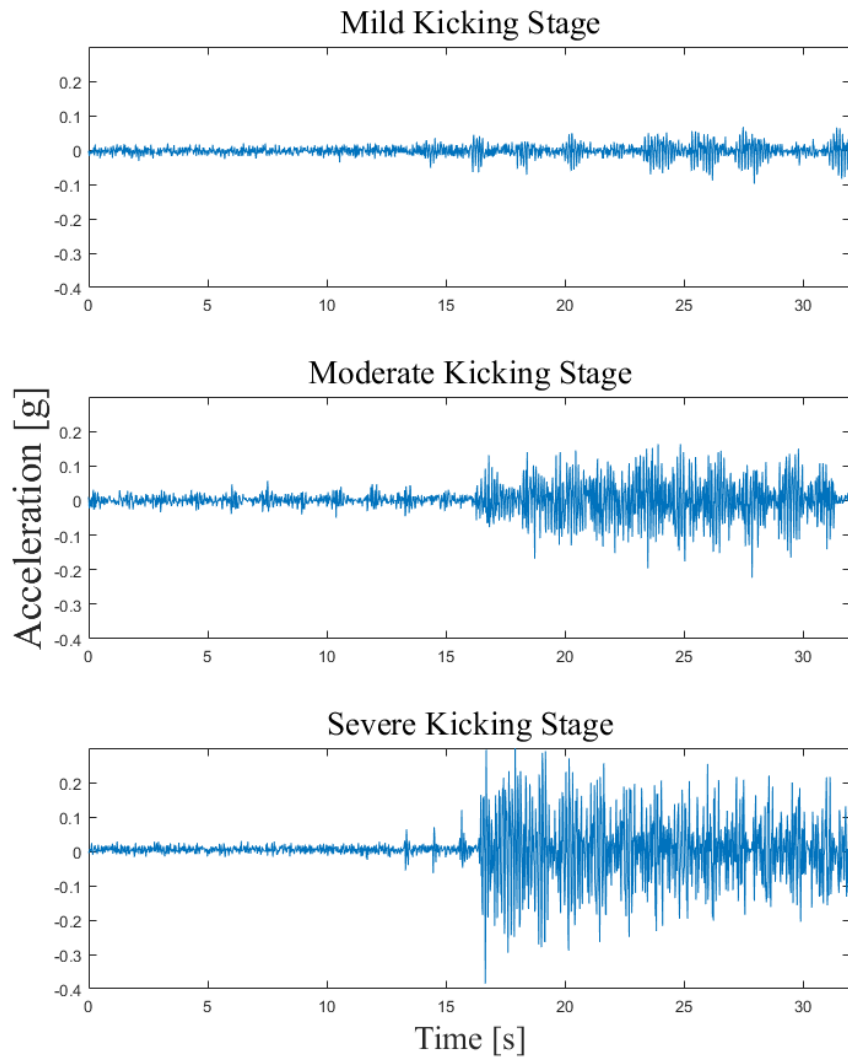


**Figure 2-4.** Waveforms of kicking phenomenon from *in vitro* mock circulation system

Kicking phenomenon was reproduced by *in vitro* mock circulation system. Figure 2-4 shows kicking phenomenon occurred at around 15 seconds with three different intensities by changing experimental settings such as resistances, compliance pressures, ECMO motor speed and heart rate of the mock circulation loop.

## 2.4 Algorithm development

Decision of an appropriate parameter is the first step of developing an algorithm. In this study, the best parameter that best reflects the moment of kicking was chosen through comparison of correlation between the candidate parameters and kicking data. Machine learning algorithm was applied for the comparison between them. The process was performed using data of 29,000 seconds which was half of the total *in vivo* data. The remaining half were used for validation of the final algorithm. Algorithm development was carried out with the parameter that was decided through the comparison.

### 2.4.1 K-Nearest Neighbor (K-NN) algorithm

K-NN algorithm is well known as a simple and an effective way of classifying various types of datasets. determines the class label based on number of its nearest neighbors. Given set  $X$  and a distance function, K-NN algorithm searches to find the number of  $k$  closest points in  $X$  to a query point or set of points. Normally, Euclidean distance function is used. But there are two other major distance functions valid for continuous variables.

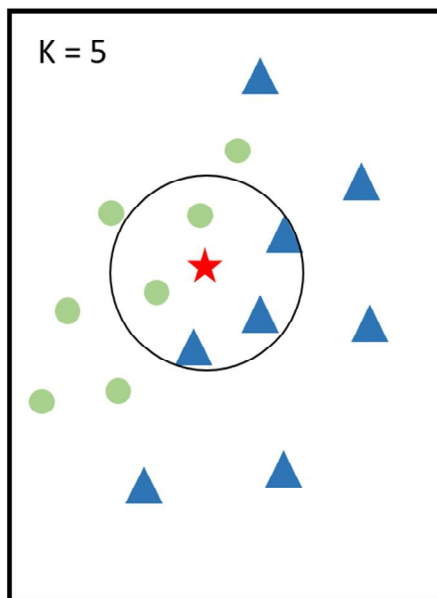
$$\text{Euclidean distance function : } \sqrt{\sum_{i=1}^k (x_i - y_i)^2} \quad (1)$$

$$\text{Manhattan distance function : } \sum_{i=1}^k |x_i - y_i| \quad (2)$$

$$\text{Minkowski distance function : } \left( \sum_{i=1}^k (|x_i - y_i|)^q \right)^{\frac{1}{q}} \quad (3)$$

It is important to find the optimal value of k. Generally, a large value of k reduces overall noise which results in more precise classification. Cross-validation is performed to validate an appropriate k value with an independent dataset. K-NN algorithm is widely used and regarded the simplest of all machine learning algorithms because it does not use training datasets to do any generalization. The principles of K-NN algorithm is visually explained in Figure 2-5. In this study, K-NN algorithm was performed with MATLAB (R2017a, Mathworks, Natick, USA) classification learner machine learning software tool box.

(a)



(b)

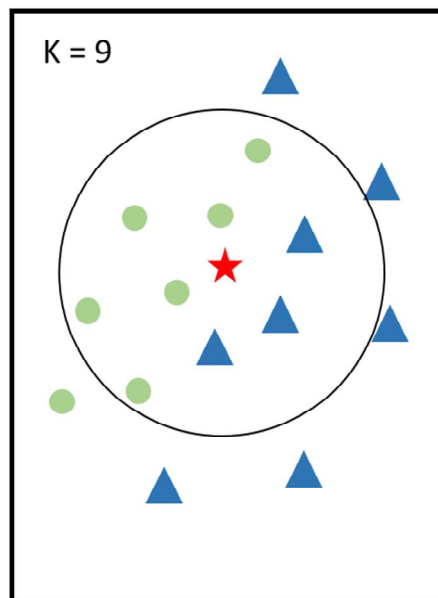


Figure 2-5. K-nearest neighbor (K-NN) algorithm

K – NN algorithm classifies the dataset by a majority of vote of neighbors. It counts k number of neighbors and the dataset is classified to the class majority of neighbor belongs to. For example, star class is classified as triangle class when k equals 5 while it is classified as circle class when k equals 9. It is thus important to find the optimal value of k since it can dramatically change the classification results.

## 2.4.2 Confusion matrix

Confusion matrix, also known as confusion table, contingency table or an error matrix, is a table that visually provides performance of an algorithm. It shows the number of correct and incorrect predictions made by the classification model compared to the actual values in the data. Classification problems using only two classes, which is called binary cases, can be evaluated by a 2 x 2 confusion matrix. Each row of the matrix represents the cases of a predicted class while each column represents the cases of an actual class resulting in four possible outcomes of the confusion matrix. Confusion matrix table is shown in Figure 2-6.

The definitions of TP, TN, FP, FN are as follows :

True positive (TP) : Positive instances that were correctly classified as positives.

True Negative (TN) : Negative instances that were correctly classified as negatives.

False Positive (FP) : Negative instances that were incorrectly classified as positives. (Type 1 error)

False Negative (FN) : Positive instances that were incorrectly classified as negatives. (Type 2 error)

There are other basic measurements from the confusion matrix. Some algorithms need to

avoid false negatives more than false positives or vice versa. For the reason, there are several evaluating measurements of the outcomes of the confusion matrix. Sensitivity, also called recall or true positive rate, relates to the classifier's ability to correctly detect positive instances. Precision refers to correctly classified positive instances among all the predicted positive cases. It is often used together with sensitivity to compute F1 score which is another measure of classifier's accuracy. Specificity refers to the classifier's ability to correctly identify negative instances. Finally, accuracy is the most common and intuitive measures derived from the confusion matrix. It is proportion of all correct predictions among the total number of the dataset. It refers to the degree to the predictions of a classifying model matching the actual class.

$$Accuracy = \frac{TN + TP}{TN + FP + FN + TP} \quad (4)$$

$$Precision = \frac{TP}{FP + TP} \quad (5)$$

$$Sensitivity = \frac{TP}{TP + FN} \quad (6)$$

$$Specificity = \frac{TN}{TN + TP} \quad (7)$$

		Predicted Class	
		False	True
Actual Class	False	True Negative	False Positive
	True	False Negative	True Positive

**Figure 2-6. Confusion matrix**

Confusion matrix is a table that visually provides performance of an algorithm. It shows the number of correct and incorrect predictions made by the classification model compared to the actual values in the data.

### 2.4.3 Parameter decision

In order to determine the parameter that best reflects kicking phenomenon, K-NN machine learning algorithm was applied. Each of four parameters from the ECMO device (Flowrate, motor rotating speed, inlet pressure, motor current consumption) were trained with golden standard data (acceleration of venous line of the ECMO circuit) respectively. Four basic outcomes of confusion matrix were used to evaluate each trained models. Sensitivity, specificity, accuracy and precision were calculated from confusion matrix of each of the trained models. From the four basic outcomes, another two measures can be obtained to evaluate performance of classifiers.

F-score, also known as F1 score or F-measure, is a measure of a test's accuracy. It considers both sensitivity and precision of the test to compute the score. F-score is harmonic mean value of sensitivity and precision. If perfect precision and sensitivity is acquired, F-score reaches 1 and worst at 0. F-score can be calculated by the following equation.

$$F\ score = 2 \cdot \frac{1}{\frac{1}{sensitivity} + \frac{1}{precision}} = 2 \cdot \frac{precision \cdot sensitivity}{precision + sensitivity} \quad (6)$$

The Matthews correlation coefficient is applied in machine learning fields as a measure of quality of binary classifiers. It was introduced by biochemist Brian W. Matthews in 1975. Matthews correlation coefficient has a range of -1 to 1 where value of 1 indicates a perfect binary classifier while value of -1 indicates a completely wrong binary classifier. The Matthews correlation coefficient was calculated by the following equation.

$$Matthews\ correlation\ coefficient = \frac{TP \cdot TN - FP \cdot FN}{\sqrt{(TP + FP)(TP + FN)(TN + FP)(TN + FN)}} \quad (7)$$

To sum up, overall six measurements were computed from the confusion matrix of the classification model trained by K-NN machine learning algorithm. By evaluating the classification models of each ECMO operation monitoring parameters, correlation between the parameters and exact moment of kicking was analyzed respectively. The overall correlation comparison process schematic was shown in Figure 2-7.

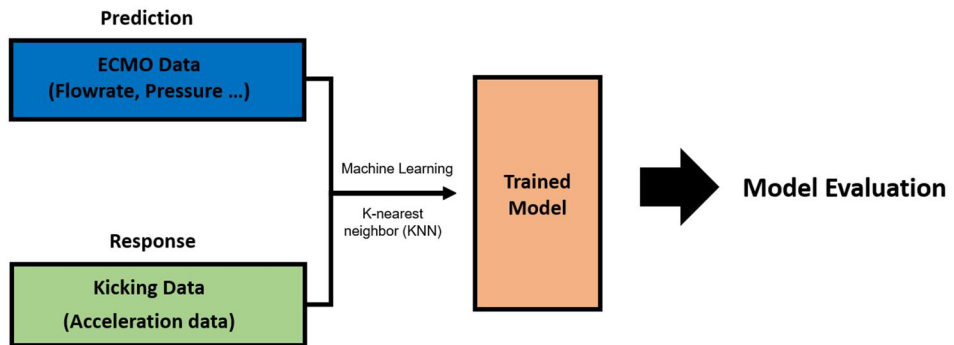


**Figure 2-7. Parameter decision process**

The best parameter that best reflects the moment of kicking phenomenon was chosen

through comparison of correlation between the candidate parameters and kicking data. Trained model performed by K-NN machine learning algorithm was evaluated for the correlation comparison.

#### 2.4.4 Algorithm decision

Three candidate algorithms were developed on the basis of the determined parameter. The three indicators were selected to detect suction moments based on the fact that kicking phenomenon leaves negative spikes on the waveforms of ECMO monitoring parameters due to instant vacuum created at the moment of drainage catheter blockage. The indicators that were utilized in suction detection systems in LVAD were applied [32]. Final algorithm was determined by analyzing accuracies of the three different algorithms through comparison between them and *in vitro* experiment data.

##### 2.4.4.1 Standard deviation algorithm

Standard deviation is a quantified measure of variation or dispersion of data. It is calculated

by square root of its variance which is the average of the squared differences from the average value. A low standard deviation value indicates the data being aggregated to the average, while a high standard deviation value indicates the data being widely spread out. ECMO data fluctuates at the instance of kicking phenomenon which leads to rise of standard deviation value of the data. The standard deviation of previous certain time period was calculated to be regarded as detection indicator.

$$Threshold < \sqrt{\frac{\sum (data\ average - curren\ data)^2}{window\ length}} \quad (8)$$

#### 2.4.4.2 Min-max algorithm

Another effective indicator for kicking can be found by the relation between the maximum and minimum values of the data. The maximum amplitude of the data increases at the kicking instances compared to normal status. In min-max algorithm, the difference between minimum and maximum value of the data were calculated. This criterion is more sensitive to the exact moment of kicking than the standard deviation algorithm.

$$Threshold < Maximum\ data - Minimum\ data \quad (9)$$

#### 2.4.4.3 Differential algorithm

Kicking moments accompany falling edges caused by instant negative pressure of the pump inlet. In the differential algorithm, kicking is detected if there exists falling edges that exceed a certain threshold level within the time window. This criterion shows the most sensitive response to the exact moment of kicking than the other two detection indicators.

$$Threshold < maximum(data\ differential) \quad (10)$$

#### 2.4.5 Window problem

Real-time suction detection algorithms require deep considerations of detecting window length decision. A longer window will provide more accurate detections but results in prolonged response of the suction event. On the contrary, a shorter window shows faster data processing but results in less accurate detections. The tradeoff should be considered to develop a detection algorithm. Previous works on suction detection algorithms applied various sized windows that vary from 2 to 6 seconds [33, 34]. One of the factors that affects the frequency of the kicking phenomenon is mechanical ventilation frequency. In situations of mechanical inspiration, increase in pleural pressure results in intravascular pressure of the right atrium and inferior vena cava. The raised pressure encourages venous collapse that leads to kicking phenomenon. For this reason, window length of slightly longer than 5 second, which is general mechanical ventilation frequency, was determined to be the most appropriate size of

the window in this study.

## **Chapter 3. Results**

### **3.1 *In vivo* experiment results**

Overall six parameters which include inlet pressure of centrifugal blood pump, flow rate, motor current, rotating speed of the blood pump and acceleration intensity which indicates moments of kicking phenomenon was collected during 24-hours operation of VA-ECMO. Figure 3-1 show the acquired data of the experiment. Red boxes refer to the time periods of kicking phenomenon occurrences. During 58000 seconds of the experiment, kicking occurred

33112 seconds. Throughout all the data, trembling of the waveforms occurred simultaneously with the onset of kicking phenomenon. The results show negative pressure of drainage line caused by venous collapse interferes with the rotating blood pump and the snatching force directly transfers to the motor through magnetic coupling between the blood pump and the motor.

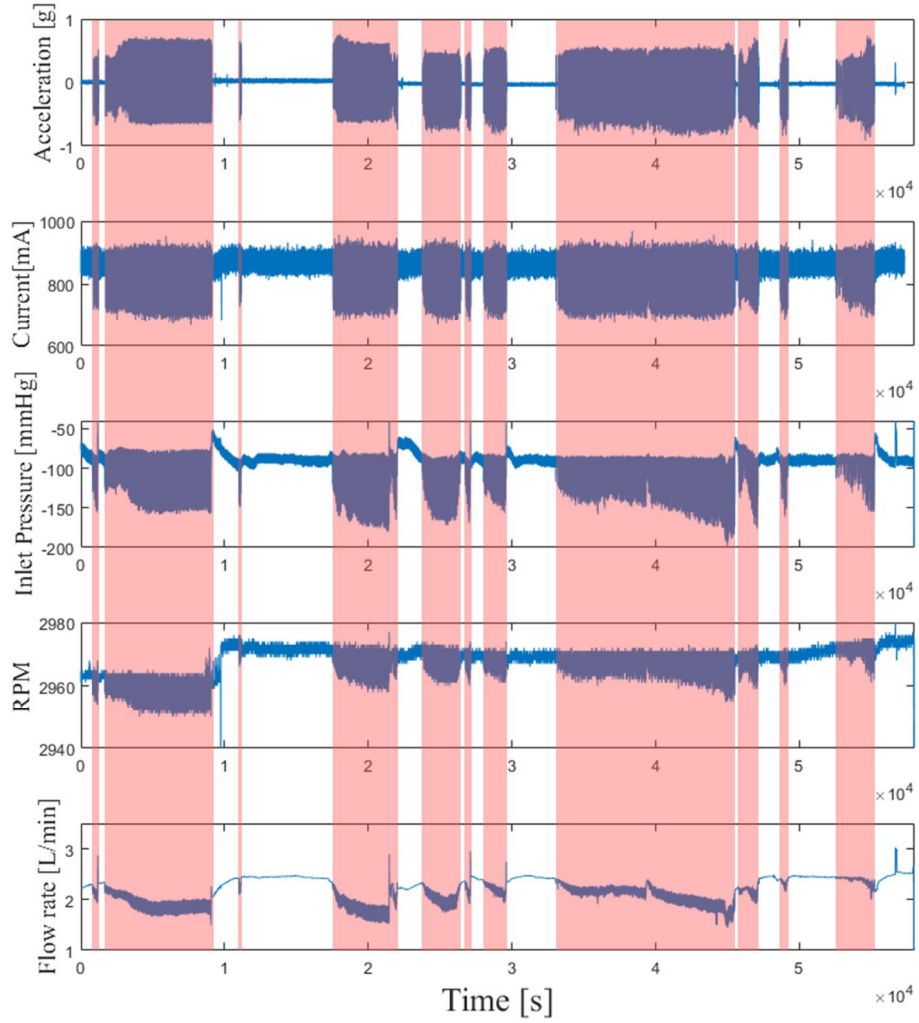


**Figure 3-1. *In vivo* experiment data outcomes**

24-hour data acquired from *in vivo* experiment. Data in the figure show data of last 16 hours.

Red boxes refer to the time periods of kicking phenomenon occurrences.

## 3.2 Correlation comparison

As mentioned in section 2.4.2, confusion matrix of machine learning algorithm classified models were evaluated to determine the parameter that best reflects kicking phenomenon. First, every ECMO monitoring parameters were linearly interpolated to synchronize time period since each parameter had different sampling rates. Figure 3-2 shows the confusion matrix of each parameters and kicking phenomenon. And table 3-1 shows the computed results of accuracy, sensitivity, precision and specificity derived from the confusion matrix. Since the instance of kicking phenomenon had occupied less than 4% of the rest of the operating periods, accuracy of all of the four parameters scored over 97%. Accuracy was judged to have insufficient discrimination ability to evaluate the algorithm. But in terms of precision and sensitivity, motor current consumption data outperformed other parameters up to almost 30%. Consequently, motor current data were considered as a parameter that best reflects kicking moments.

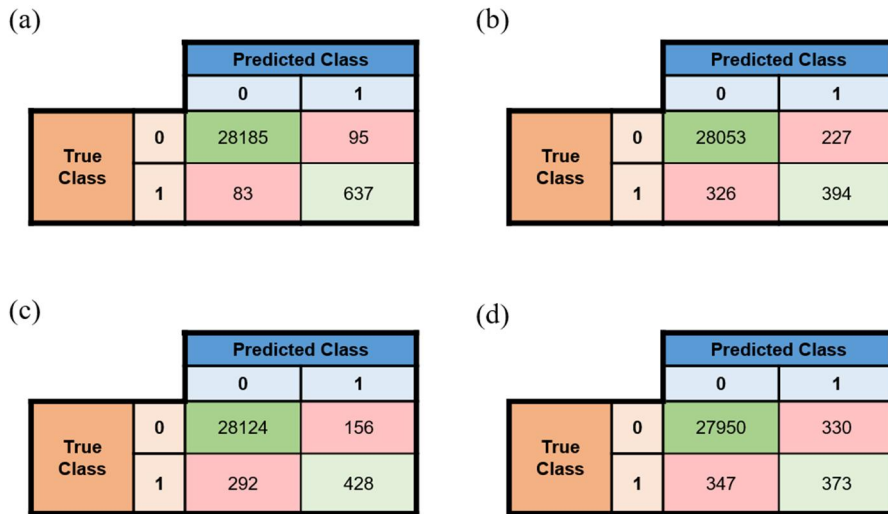


**Figure 3-2. Confusion matrix of the candidate parameters**

Confusion matrix of candidate parameters. (a) motor current data (b) flow rate data (c) drainage pressure data (d) pump rotating speed data

	Accuracy	Precision	Sensitivity	Specificity
Current	99.4	87.0	88.5	99.7
Flowrate	98.1	63.4	54.7	99.1
Inlet Pressure	98.4	73.3	59.4	99.4
RPM	97.6	53.1	51.8	98.8

**Table 3-1. Confusion matrix outcomes**

Outcomes of the attained confusion matrix of the candidate parameters were calculated to evaluate the correlation between the parameters and kicking phenomenon.

### 3.3 *In vitro* evaluation

In-vitro algorithm evaluations of the three candidate algorithms were performed using mock circulation system which was explained in section 2.3. Data acquired from the mock circulation system was shown in Figure 3-3. The *in vitro* ECMO data has shown waveforms that were very similar to the *in vivo* ECMO data. Motor current, drainage catheter pressure and rotating speed data waveforms has trembled at the instance of kicking phenomenon which corresponds to *in vivo* experiment data while flow rate data has only decreased without trembling. Algorithm evaluation was performed using *in vitro* mock circulation system since *in vitro* experiments have the advantage of being able to acquire results of various experimental conditions. Therefore, the algorithm can be evaluated in various kicking situations which might occur in actual ECMO operations.

Three suction detection indicators were developed based on the basis of the motor current data. Each algorithm developed with the three indicators were evaluated by *in vitro* kicking experiment data acquired in conditions of different kicking intensities. Figure 3-4~6 show the algorithm application results of kicking conditions of different acceleration intensities induced deliberately by *in vitro* mock circulation system. Each kicking conditions show difference in waveforms of motor current consumption. In mild kicking stages, which accompanies a slight trembling of the circuit, current consumption waveforms get slightly lower at the instance of mild kicking. On the other hand, in severe kicking stages which violent tremors are observed, motor current consumption data waveform can be clearly distinguished at the instance of severe kicking event. As seen in Figure 3-4, all of the three candidate algorithms had difficulty detecting the kicking event during mild kicking stage where the current data fluctuation is not significant. In contrast, as the kicking intensity increased from moderate to severe, all the three candidate algorithms detected kicking events better. Table 3-2 show the results of quantitative

analysis of the detection capabilities of each candidate algorithms in each of the stages. The algorithm developed based on standard deviation values had best detection capabilities than the other two candidate algorithms throughout all the kicking stages. Especially, in moderate kicking stage, standard deviation algorithm showed 82.9% in sensitivity outperforming other two algorithms which showed only 34% in sensitivity. The algorithm using standard deviation values were chosen as the final suggested algorithm since it stably performs detection of kicking events in various kicking environments.

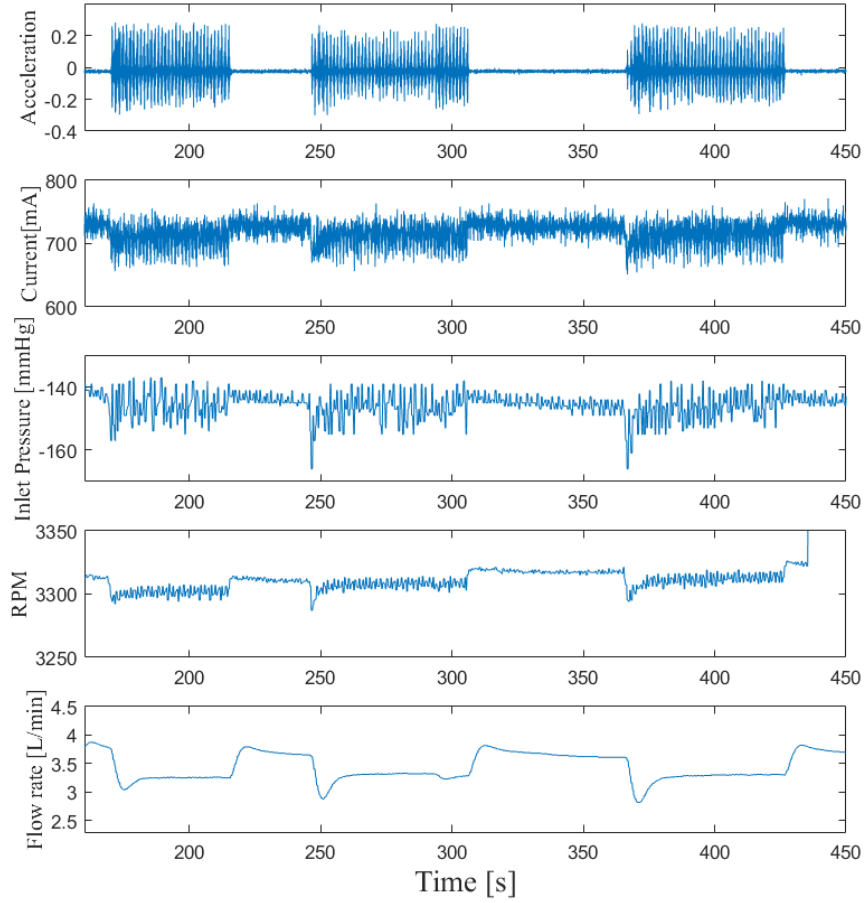


**Figure 3-3. Kicking data acquired from mock circulation system**

Data from mock circulation system, which was used to validate the suggested algorithm, was acquired. The waveforms during kicking situations acted similar to the *in vivo* experiment result.

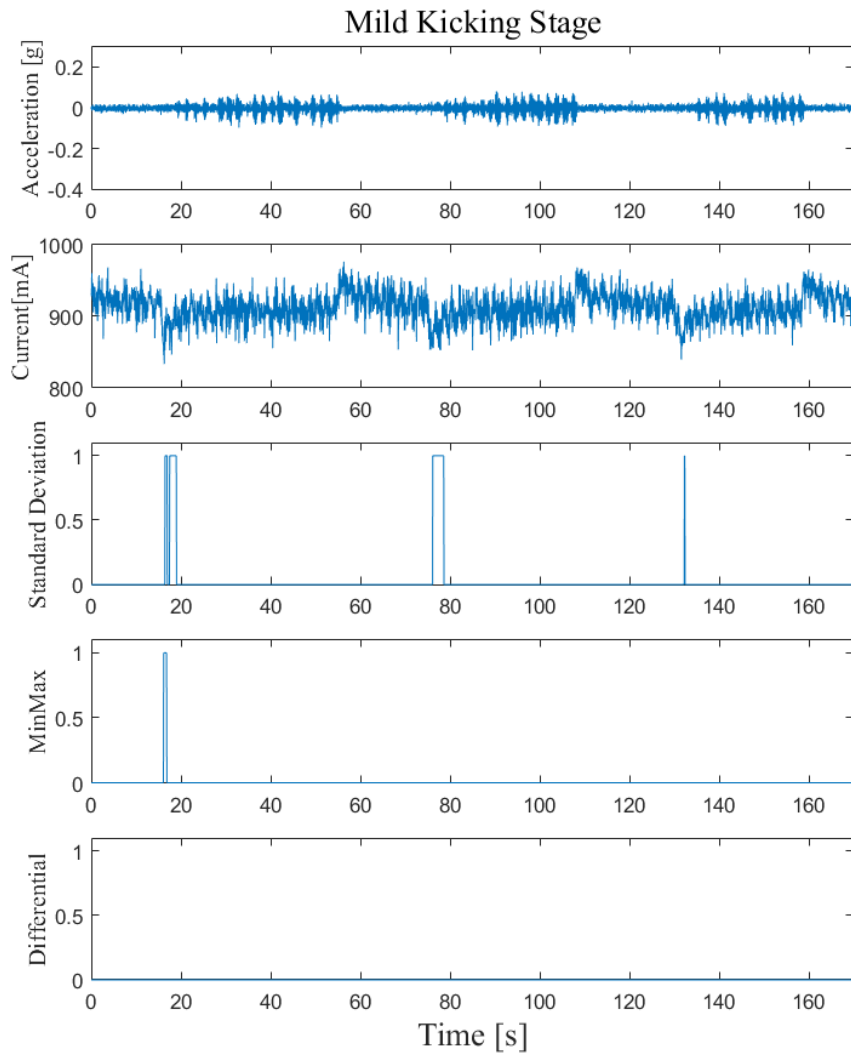


**Figure 3-4. Algorithm application results during mild kicking stage**

It was classified as mild kicking stage when the acceleration level was 0.08 g or less, which is a slight trembling that can be seen just before kicking occurs in earnest.

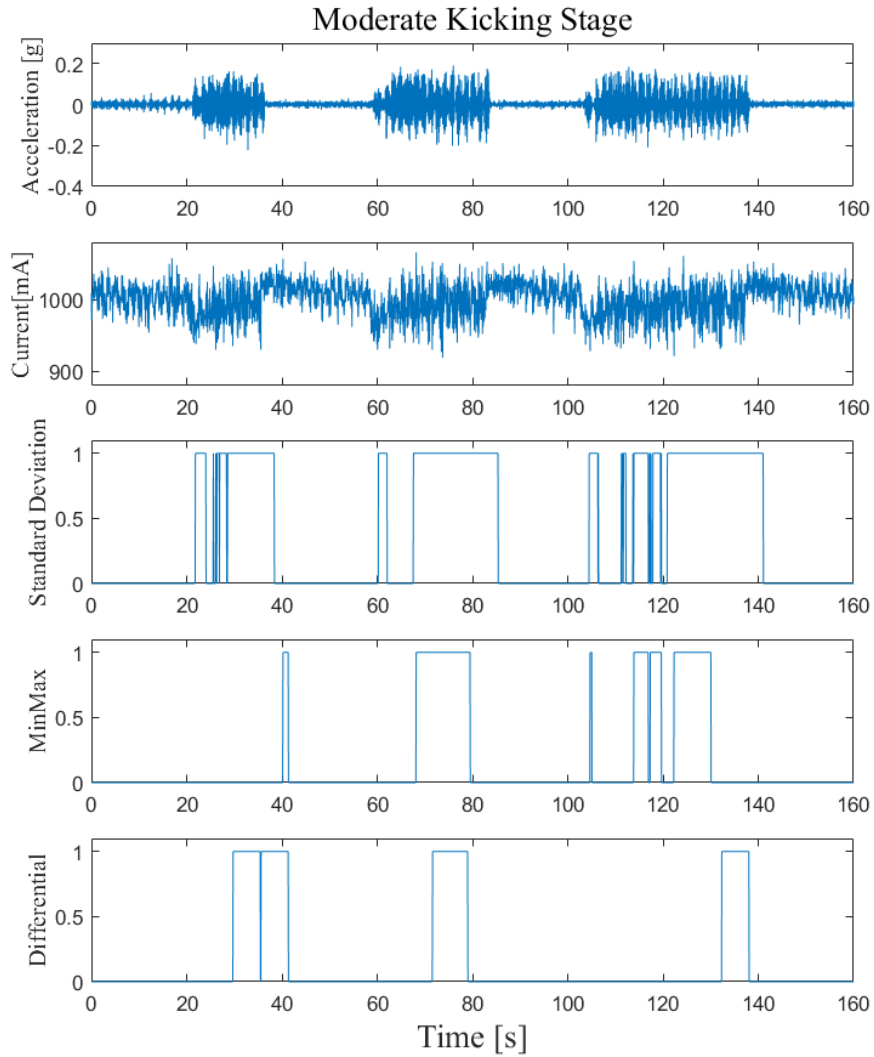


**Figure 3-5. Algorithm application results during moderate kicking stage**

It was classified as moderate kicking stage when the acceleration level was in the range of 0.08 to 0.16 g which accompanies a noticeable shaking of the circuit as the kicking phenomenon progresses.

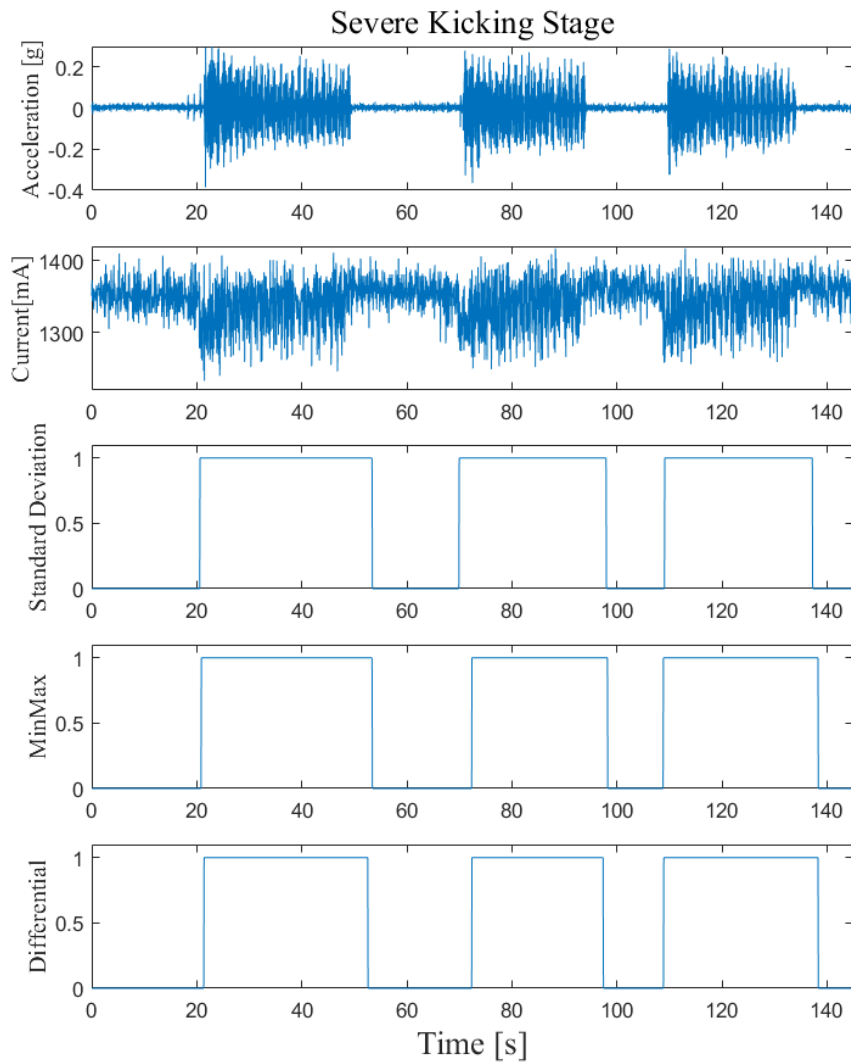


**Figure 3-6. Algorithm application results during severe kicking stage**

It was classified as severe kicking stage when the acceleration level reached 0.16 g or more.

Violent tremors can be observed at the instance of severe kicking

	Mild		Moderate		Severe	
	Accuracy	Sensitivity	Accuracy	Sensitivity	Accuracy	Sensitivity
Standard Deviation	50.6	7.1	91.9	82.9	98.0	97.1
Minmax	47.2	1.2	68.8	34.2	97.6	96.2
Differential	46.9	0	69.1	34.9	97.5	96.0

**Table 3-2. Algorithm evaluation results during different kicking stages**

Results of quantitative analysis of the detection capabilities of each candidate algorithms in each of the stages. The algorithm developed based on standard deviation values had best detection capabilities than the other two candidate algorithms throughout all the kicking stages.

### 3.4 The suggested algorithm

Determining an adequate parameter and indicator to detect kicking phenomenon was performed in previous sections. Deciding an adequate level of threshold is another crucial consideration to be made. Different threshold should be applied because every patient has different physiological characteristics and every cannula insertion surgery encounters different situations. Therefore, adaptive thresholding was applied in the detection algorithm. As soon as a first incoming datum is acquired from the ECMO device, it is checked if ECMO operation is in a steady state to make sure it is ready to detect kicking phenomenon. Once it is certified to be steady, threshold level is set to the average value of current standard deviation. Afterwards, the incoming data are calculated and compared with the threshold level to be decided whether it is currently on kicking situation or not. The final kicking detection algorithm block diagram is shown in Figure 3-7.

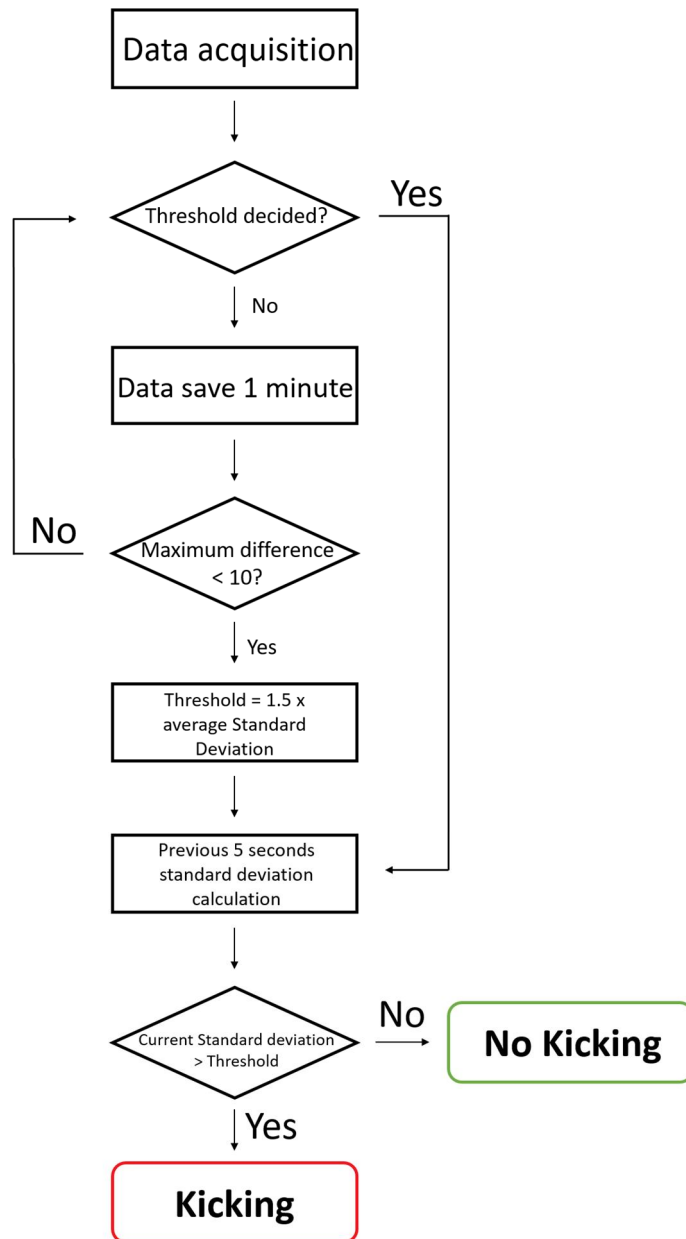


**Figure 3-7. Block diagram of the suggested algorithm**

Final kicking detection algorithm was presented. Adaptive thresholding was applied to consider different physiological characteristics of each patient.

## Chapter 4. Discussion

### 4.1 Algorithm validation

The suggested kicking detection algorithm was finally validated with *in vivo* experiment data. The validation process was performed on the other half of the total data which excludes the data used for parameter selection. The reference data used as validation was 29000 seconds which corresponds to 8 hours of kicking data. The suggested kicking detection algorithm was applied to the data and were analyzed by comparing the detection result to actual kicking moment recorded with acceleration level of the ECMO circuit. Figure 4-1 show the result of actual kicking phenomenon and the detection result of the suggested algorithm. The analyzed data was set out in a confusion matrix which can be seen in Figure 4-2 and the outcomes are shown in Table 4-1. The suggested kicking detection algorithm showed 97.6% in accuracy, 99.5% in precision, 96% sensitivity and 99.4% in specificity. These results indicate significant detecting performance as shown in Table 4-1.

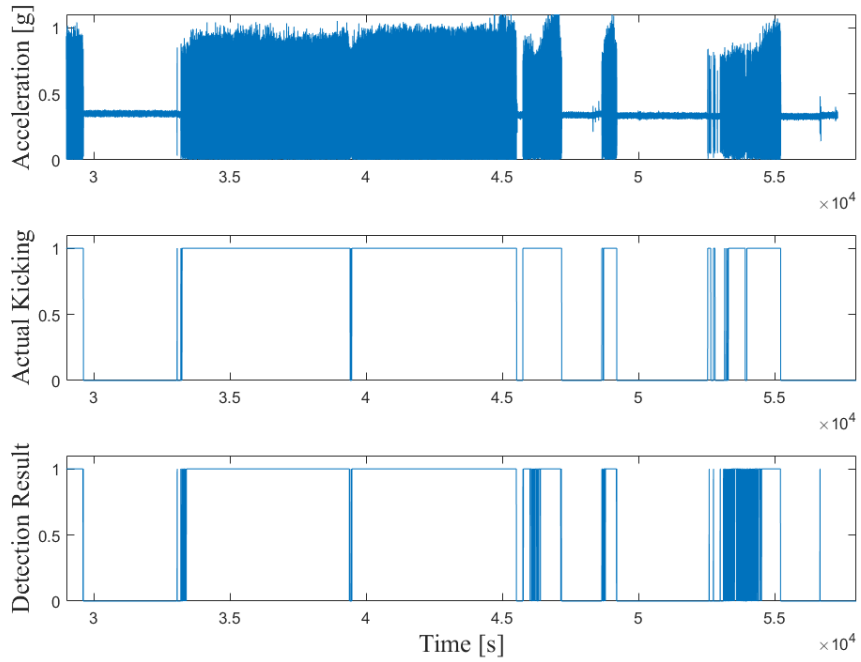


**Figure 4-1. *In vivo* experiment data application results of suggested kicking detection algorithm**

The detection results of the suggested kicking detection algorithm were compared with the actual kicking data acquired from acceleration levels of the ECMO circuit.

		Predicted Class	
		0	1
True Class	0	12373	73
	1	615	15941

**Figure 4-2. Confusion matrix of detection results using suggested kicking detection algorithm**

The figure shows a confusion matrix of the detection results of actual kicking events from *in vivo* experiment data using suggested kicking detection algorithm.

Algorithm Detection Performance	
<b>Accuracy</b>	97.6
<b>Precision</b>	99.5
<b>Sensitivity</b>	96.3
<b>Specificity</b>	99.4

**Table 4-1. Confusion matrix outcomes of the suggested kicking detection algorithm**

Outcomes of the attained confusion matrix were calculated to evaluate the performance of the suggested kicking detection algorithm. The results indicate significant detection performance.

## 4.2 Feasibility of the suggested algorithm on ECMO devices

In this study, motor current data were judged to best reflect kicking phenomenon among several different parameters from the developed ECMO device. Therefore, the suggested algorithm adopted motor current parameter as an indicator for kicking detection. There are several advantages of using motor current parameter as kicking detection in ECMO operations other than the accuracy of the algorithm itself. Other parameters such as drainage pressure and flow rate, it is necessary to equip additional sensors on the ECMO circuit. However, measurement of motor current does not require additional sensors which leads to simplification of the ECMO circuit. Also clinicians might inject drugs or take blood samples to check patient's status through the pressure line on ECMO operations. Kicking detection using pressure data is restricted during those kind of situations while acquiring motor current data never be disrupted unless the motor turns off.

### 4.3 Limitations of the present study

There are some limitations that were unable to overcome in the present study. The limitations include number of *in vivo* experiment subjects, lack of clinician's opinion during the process of algorithm development, dissimilarities between actual ECMO operations and mock circulation system and lack of algorithm validation with other ECMO devices. These problems are closely analyzed and will be improved in the further studies.

First, the number of subject was too small for algorithm development. There is a possibility of some unique kicking situations that exist in other subjects. Various data acquired from large number of subject is required to increase credibility of the kicking detection algorithm in the future work.

Second, opinions of clinicians were insufficiently reflected while developing the detection algorithm. Clinicians such as perfusionists and nurses are the people who actually demand this detection algorithm. Usability of the algorithm should be considered by gathering and understanding their needs.

Third, the mock circulation system that were used evaluating the kicking detection algorithm could not perfectly reflect physiological characteristics of the in-vivo ECMO experiment. Although blood viscosity was reflected by certain proportion of glycerol addition to the mock circulation circuit, it would act differently since blood is a non-Newtonian fluid which changes in viscosity depending on shear rates while glycerol added water is a Newtonian fluid that does not change in viscosity depending on different shear rates. In some studies, whole bovine blood or human red blood cell (RBC) suspension was applied to solve these problems [35]. Thus, using non-Newtonian fluid such as whole blood and RBC suspension might be an option for future trial. Also, properties of vein model do not perfectly match the mechanical

properties of actual vein. This may result in different outcomes of venous collapse situations. Applying vein model that has identical mechanical properties with the actual drainage vein and supplement of other compartments that represent human physiology during ECMO operations will improve mock circulation system performance.

Finally, the algorithm was not validated in other commercial ECMO devices. The parameters used for establishment of the detection algorithm were carried out with only with the self-developed ECMO device. Therefore, the algorithm should be tested in other commercial ECMO devices in order to certify this algorithm is valid for every ECMO operations.

## Chapter 5. Conclusion

In this study, a kicking detection algorithm that utilizes a parameter that best reflects the kicking situation was introduced. The parameter that best reflects kicking situation was selected by K-NN machine learning algorithm and the accuracy of different algorithms developed based on the selected parameter was analyzed in different kicking intensities induced by *in vitro* mock circulation system to determine the final kicking detection algorithm.

The developed kicking detection algorithm had about 97% accuracy and sensitivity on in-vivo experiment data. Lack of test data set of in-vivo experiment data is an obstacle for the confidence of the detection algorithm. Nevertheless, it can be solved by validating the detection system during in-vivo experiments which will be performed in further studies.

Even though there remain some limitations in this research, it still has great possibility to be applied in other ECMO operations. Since there are insufficient studies of suction detection system during ECMO operations currently, this study might be a foundation of suction detection system on various ECMO operating situations.

## References

- [1] Sanders, C. A., Buckley, M. J., Leinbach, R. C., Mundth, E. D., & Austen, W. G., “Mechanical circulatory assistance.”, *Circulation*, vol. 45(6), pp. 1292-1313, 1972.
- [2] Cooley, D. A., “The total artificial heart.”, *Nature medicine*, vol. 9(1), pp. 108-111, 2003.
- [3] Rose, E. A., Gelijns, A. C., Moskowitz, A. J., Heitjan, D. F., Stevenson, L. W., Dembitsky, W., ... & Watson, J. T., “Long-term use of a left ventricular assist device for end-stage heart failure.”, *New England Journal of Medicine*, 345(20), 1435-1443, 2001.
- [4] Copeland, J. G., Smith, R. G., Arabia, F. A., Nolan, P. E., Sethi, G. K., Tsau, P. H., ... & Slepian, M. J., “Cardiac replacement with a total artificial heart as a bridge to transplantation.”, *New England Journal of Medicine*, vol. 351(9), pp. 859-867, 2004.
- [5] Ginat, D., Massey, H. T., Bhatt, S., & Dogra, V. S., “Imaging of mechanical cardiac assist devices.” *Journal of clinical imaging science*, vol. 1, 2011.
- [6] Brodie, D., & Bacchetta, M., “Extracorporeal membrane oxygenation for ARDS in adults.”, *New England Journal of Medicine*, vol. 365(20), pp. 1905-1914, 2011.
- [7] Shekar, K., Gregory, S. D., & Fraser, J. F., “Mechanical circulatory support in the new era: an overview.”, *Critical Care*, vol. 20(1), pp. 66, 2016.
- [8] Kolff, W. J., Berk, H. T. H. J., Welle, N. M., Ley, A. J. W., Dijk, E. C., & Noordwijk, J., “The artificial kidney: a dialyser with a great area.”, *Journal of Internal Medicine*, vol. 117(2), pp. 121-134, 1944.
- [9] GIBBON Jr, J. H., “Application of a mechanical heart and lung apparatus to cardiac surgery.”, *Minn med*, vol. 37, pp. 171-185, 1954.

- [10] Bartlett, R. H., Gazzaniga, A. B., Jefferies, M. R., Huxtable, R. F., Haiduc, N. J., & Fong, S. W., "Extracorporeal membrane oxygenation (ECMO) cardiopulmonary support in infancy.", *ASAIO Journal*, vol. 22(1), pp. 80-92, 1976.
- [11] Sievert, A. N., Shackelford, A. G., & McCall, M. M., "Trends and emerging technologies in extracorporeal life support: results of the 2006 ECLS survey.", *The Journal of extra-corporeal technology*, vol. 41(2), pp. 73, 2009.
- [12] DeLaney, E., Smith, M. J., Harvey, B. T., Pelletier, K. J., Aquino, M. P., Stone, J. M., ... & Johnson, J. H., "Extracorporeal life support for pandemic influenza: the role of extracorporeal membrane oxygenation in pandemic management.", *The journal of extra-corporeal technology*, vol. 42(4), pp. 268, 2010.
- [13] Lequier, L., Horton, S. B., McMullan, D. M., & Bartlett, R. H., "Extracorporeal membrane oxygenation circuitry.", *Pediatric critical care medicine: a journal of the Society of Critical Care Medicine and the World Federation of Pediatric Intensive and Critical Care Societies*, vol. 14(5 0 1), pp. S7, 2013.
- [14] Seal, P. F., "Mechanical Ventilation: Clinical Applications and Pathophysiology.", *Anaesthesia and Intensive Care*, vol. 36(3), pp. 467-468, 2008.
- [15] Rigatti, R. L., & Stewart, R., "Heat exchange in extracorporeal systems.", *Cardiopulmonary bypass Principles and techniques of extracorporeal circulation*, pp. 247-256, 1995.
- [16] Khodeli, N., Chkhaidze, Z., Partsakhashvili, J., Pilishvili, O., & Kordzaia, D., "Practical and Theoretical Considerations for ECMO System Development.", *Extracorporeal Membrane Oxygenation-Advances in Therapy*, InTech, 2016.
- [17] Makdisi, G., & Wang, I. W., "Extra Corporeal Membrane Oxygenation (ECMO) review of a lifesaving technology.", *Journal of thoracic disease*, vol. 7(7), pp.E166,

2015.

- [18] Sidebotham, D., McGeorge, A., McGuinness, S., Edwards, M., Willcox, T., & Beca, J., “Extracorporeal membrane oxygenation for treating severe cardiac and respiratory failure in adults: part 2—technical considerations.”, *Journal of cardiothoracic and vascular anesthesia*, vol. 24(1), pp. 164-172, 2010.
- [19] Cirri, S., Negri, L., Babbini, M., Latis, G., Khlat, B., Tarelli, G., ... & Bordignon, F., “Haemolysis due to active venous drainage during cardiopulmonary bypass: comparison of two different techniques.”, *Perfusion*, vol. 16(4), pp. 313-318, 2001.
- [20] Pedersen, T. H., Videm, V., Svennevig, J. L., Karlsen, H., Østbakk, R. W., Jensen, Ø., & Mollnes, T. E., “Extracorporeal membrane oxygenation using a centrifugal pump and a servo regulator to prevent negative inlet pressure.”, *The Annals of thoracic surgery*, vol. 63(5), pp. 1333-1339. 1997.
- [21] Tulman, D. B., Stawicki, S. P., Whitson, B. A., Gupta, S. C., Tripathi, R. S., Firstenberg, M. S., ... & Papadimos, T. J. “Veno-venous ECMO: a synopsis of nine key potential challenges, considerations, and controversies.”, *BMC anesthesiology*, vol. 14(1), pp. 65, 2014.
- [22] Martin, G. S., Moss, M., Wheeler, A. P., Mealer, M., Morris, J. A., & Bernard, G. R., “A randomized, controlled trial of furosemide with or without albumin in hypoproteinemic patients with acute lung injury.”, *Critical care medicine*, vol. 33(8), pp. 1681-1687, 2005.
- [23] Schima, H., Trubel, W., Moritz, A., Wieselthaler, G., Stohr, H. G., Thoma, H., ... & Wolner, E., “Noninvasive monitoring of rotary blood pumps: Necessity, possibilities, and limitations.”, *Artificial Organs*, vol. 16(2), pp. 195-202, 1992.
- [24] Tsukiya, T., Taenaka, Y., Nishinaka, T., Oshikawa, M., Ohnishi, H., Tatsumi, E., ... & Shimada, M., “Application of indirect flow rate measurement using motor

- driving signals to a centrifugal blood pump with an integrated motor.”, *Artificial organs*, vol. 25(9), pp. 692-696, 2001.
- [25] Yuhki, A., Hatoh, E., Nogawa, M., Miura, M., Shimazaki, Y., & Takatani, S., “Detection of suction and regurgitation of the implantable centrifugal pump based on the motor current waveform analysis and its application to optimization of pump flow.”, *ARTIFICIAL ORGANS-OHIO*-, vol. 23, pp. 532-537, 1999.
- [26] Fu, M., & Xu, L., “Computer simulation of sensorless fuzzy control of a rotary blood pump to assure normal physiology.”, *Asaio Journal*, vol. 46(3), pp. 273-278, 2000.
- [27] Saito, I., Ishii, K., Isoyama, T., Ono, T., Nakagawa, H., Shi, W., ... & Abe, Y., “Preliminary study of physiological control for the undulation pump ventricular assist device.”, *Engineering in Medicine and Biology Society (EMBC), 2010 Annual International Conference of the IEEE* (pp. 5218-5221). IEEE, 2010.
- [28] Mitaka, C., Nagura, T., Sakanishi, N., Tsunoda, Y., & Amaha, K., “Two-dimensional echocardiographic evaluation of inferior vena cava, right ventricle, and left ventricle during positive-pressure ventilation with varying levels of positive end-expiratory pressure.”, *Critical care medicine*, vol. 17(3), pp. 205-210, 1989.
- [29] Barbier, C., Loubières, Y., Schmit, C., Hayon, J., Ricôme, J. L., Jardin, F., & Vieillard-Baron, A., “Respiratory changes in inferior vena cava diameter are helpful in predicting fluid responsiveness in ventilated septic patients.”, *Intensive care medicine*, vol. 30(9), pp. 1740-1746, 2004.
- [30] Yoshizawa, M., Sato, T., Tanaka, A., Abe, K. I., Takeda, H., Yambe, T., ... & Nosé, Y., “Sensorless estimation of pressure head and flow of a continuous flow artificial heart based on input power and rotational speed.”, *ASAIO journal*, vol. 48(4), pp. 443-448, 2002.

- [31] Powers, D. M., "Evaluation: From precision recall and F-factor to roc informedness markedness and correlation", *Journal of Machine Learning Technologies*, vol. 2, no. 1, pp. 37-63, 2011.
- [32] Vollkron, M., Schima, H., Huber, L., Benkowski, R., Morello, G., & Wieselthaler, G., "Development of a suction detection system for axial blood pumps.", *Artificial organs*, vol. 28(8), pp. 709-716, 2004.
- [33] Ferreira, A., Simaan, M. A., Boston, J. R., & Antaki, J. F., "Frequency and time-frequency based indices for suction detection in rotary blood pumps.", *Acoustics, Speech and Signal Processing, 2006. ICASSP 2006 Proceedings. 2006 IEEE International Conference on*, Vol. 2, IEEE, 2006.
- [34] Karantonis, D. M., Cloherty, S. L., Lovell, N. H., Mason, D. G., Salamonsen, R. F., & Ayre, P. J., "Noninvasive detection of suction in an implantable rotary blood pump using neural networks.", *International Journal of Computational Intelligence and Applications*, vol. 7(03), pp. 237-247, 2008.
- [35] Okahara, S., Tsuji, T., Ninomiya, S., Miyamoto, S., Takahashi, H., Soh, Z., & Sueda, T., "Hydrodynamic characteristics of a membrane oxygenator: modeling of pressure-flow characteristics and their influence on apparent viscosity.", *Perfusion*, vol. 30(6), pp. 478-483, 2015.

## 국문 초록

# 체외막산소화장치에서의 키텅 감지 알고리즘 개발

김현수

서울대학교 대학원

협동과정 바이오엔지니어링 전공

체외막산소화장치는 심폐기능이 정상적이지 않은 환자의 심장과 폐의 역할을 대신하여 체외막형 산화기를 통해 혈액에 산소를 공급하여 순환기 기능을 보조하는 장치이다. 키텅 현상은 정맥 협착으로 인해 흡인 캐뉼러가 막히며 혈액 펌프에 일시적인 진공 상태를 유발하여 공동현상, 용혈 및 펌핑 효율의 저하를 초래한다. 키텅 현상 감지에 관한 이전 연구들은 완전 이식형 인공심장 및 심실 보조장치와 같은 이식형 혈액펌프들에 집중되어 있어 체외막산소화장치에서의 키텅 감지 시스템의 개발에 관한 연구가 필요한 상황이다.

본 연구의 목표는 체외막산소화장치에서의 키텅 현상을 감지하는 알고리즘을 개발하는 것이다. 이를 위해 체외막산소화장치 작동 상황에서의 유속, 펌프 회전

속도, 모터의 전류 소비량, 흡인 회로에서의 압력을 킁 감지 알고리즘 개발에 사용될 후보군으로 선정하였고, 암컷 돼지에게 정맥 - 동맥 체외막산화기를 장착한 상황에서 킁 현상 시 후보 데이터들의 파형을 24시간 동안 기록하였다. 얻어진 후보 데이터들과 흡인 회로에 장착된 가속도센서를 통해 기록된 킁 현상 발생 데이터를 기계학습하여 얻어진 모델의 혼동행렬의 정확도를 평가함으로써 각 후보 데이터들과 킁 현상의 상관관계를 비교 분석하였다. 모터의 전류 소비 데이터는 민감도와 정밀도 측면에서 다른 후보 데이터들에 비해 50% 이상 높은 수치를 보였다. 모터의 전류 소비 데이터를 사용하여 여러 알고리즘을 개발하였고, 표준 편차를 이용한 알고리즘은 시험관내 실험에서 다양한 실험 조건을 변화시켜 발생시킨 여러 강도의 킁들도 가장 안정적으로 감지하여 최종 알고리즘으로 선정되었다. 제안된 최종 알고리즘은 실제 킁 데이터에 적용시켰을 때 또한 97%의 정확도를 보여 실제 체외막산소화장치에 적용 가능성을 확인하였다.

최종 알고리즘으로 선정된 모터 전류 소비 데이터는 알고리즘 자체의 정확성 이외에도 몇가지 장점을 지니고 있다. 유속이나 흡인 회로의 압력과 같은 다른 데이터의 수집을 위해서는 체외막산소화장치 회로에 추가적인 센서 장착이 요구되는 반면 모터 전류를 사용할 경우 추가적인 센서 장착이 불필요하고 모터에 전원 공급이 차단되지 않는 한 데이터 수집의 연속성이 보장된다.

본 연구에서 개발한 알고리즘은 부족한 실험 데이터로 인한 신뢰성 검증의 한계점이 존재하지만, 얻어진 결과 데이터는 체외막산소화장치에서의 킁 감지 시스템에 대한 기초연구로써 가치를 가지고 향후 더욱 정교한 알고리즘 개발의 잠재성을 시사한다.

---

주요어 : 심폐순환보조장치, 체외막산소화장치, 흡인 감지 시스템, 기계 학습, 모

의 순환 장치

학 번 : 2016-21168